Parameters vs FLOPs: Scaling Laws for Optimal Sparsity for Mixture-of-Experts Language Models

Samira Abnar*
Apple

Harshay Shah*†
MIT

Dan Busbridge
Apple

Alaaeldin Mohamed Elnouby Ali
Apple

Josh Susskind
Apple

Vimal Thilak*
Apple

Abstract

Scaling the capacity of language models has consistently proven to be a reliable approach for improving performance and unlocking new capabilities. Capacity can be primarily defined by two dimensions: the number of model parameters and the compute per example. While scaling typically involves increasing both, the precise interplay between these factors and their combined contribution to overall capacity remains not fully understood. We explore this relationship in the context of sparse Mixture-of-Expert models (MoEs), which allow scaling the number of parameters without proportionally increasing the FLOPs per example. We investigate how varying the sparsity level, i.e., the fraction of inactive parameters, impacts model's performance during pretraining and downstream evaluation. We find that under different constraints (e.g., parameter size and total training compute), there is an optimal level of sparsity that improves both training efficiency and model performance. These results provide a better understanding of the impact of sparsity in scaling laws for MoEs and complement existing works in this area, offering insights for designing more efficient architectures.

1 Introduction

Empirical scaling laws for language model pretraining (Kaplan et al., 2020; Hoffmann et al., 2022; OpenAI, 2023; 2024; Gemini Team et al., 2024; Henighan et al., 2020; Clark et al., 2022; Yun et al., 2024; Ludziejewski et al., 2024) have demonstrated that proportionally increasing model capacity, along with data and total compute budget, consistently decreases pretraining loss (i.e., perplexity), improves downstream task performance (Devlin et al., 2019; Brown et al., 2020; BIG-bench authors, 2023) and unlocks emergent capabilities (Wei et al., 2022a). While these studies typically quantify model capacity via total parameter count, *compute per example (i.e., a fixed-sized input)*, measured in FLoating OPerations (FLOPs), also plays a significant role (Clark et al., 2022). Several mechanisms (Shazeer et al., 2017; Dehghani et al., 2019; Wei et al., 2022b; Goyal et al., 2024; Csord'as et al., 2024) have been proposed that allow for independent variation of total parameter count or FLOPs within a model. For instance, Sparse Mixture-of-Experts (MoE) models (Shazeer et al., 2017) introduce "FLOP-free parameters" by leveraging sparsity, where only a subset of expert modules is activated for each input. Given this scenario where the number of parameters and FLOPs per example are not directly linked, we ask: *"Can we draw scaling laws for the optimal trade-off between parameter count and FLOPs per example?"*

To address this question, we study sparse Mixture-of-Expert Transformers (MoEs) (Shazeer et al., 2017; Lepikhin et al., 2021; Fedus et al., 2022; Zoph et al., 2022; Muennighoff et al.,

*Core contributors. Send correspondence to {abnar, vthilak}@apple.com.
†Work done while interning at Apple.

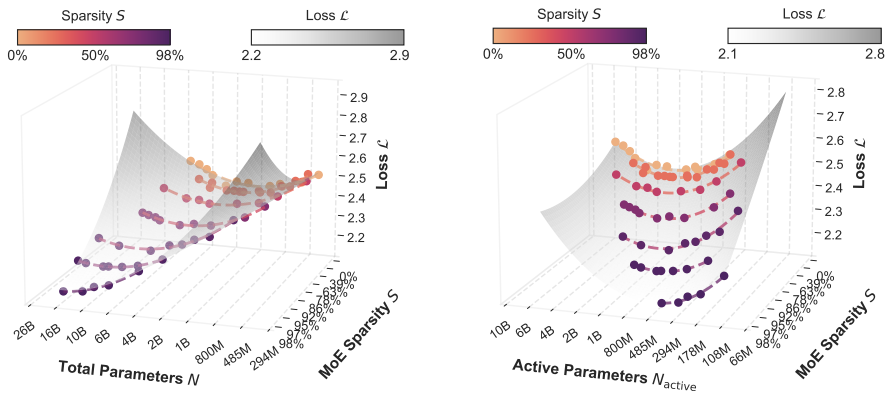

(a) IsoFLOP surface over sparsity and total parameters

(b) IsoFLOP surface over sparsity and active parameters

Figure 1: **IsoFLOP surface over observed pretraining loss L, model size (in terms of total N and active parameters $\mathbf{N_a}$), and sparsity S.** We fit a polynomial function mapping **N** (or $\mathbf{N_a}$), **S**, and their interaction to **L**, using empirical data. For both fits the MSE loss for predicting loss on a held out set is 0.0001. These results indicate that for a fixed compute budget, increasing model sparsity leads to a reduction in pretraining loss. When considering optimal model size, we observe opposite trends for total parameters (**N**) (Figure a) versus active parameters ($\mathbf{N_a}$) (Figure b). (See Figure 6 in Appendix F.3 for results with different total compute budgets C.)

2024) in the context of language modeling. Existing scaling law studies for MoEs, investigate the role of variables like number and granularity (Ludziejewski et al., 2024)of experts, underlying dense model size and inference compute in predicting the performance of the models under different conditions such as training or inference compute optimality (Du et al., 2021; Clark et al., 2022; Yun et al., 2024; Ludziejewski et al., 2024). In this paper, we focus on the interaction between FLOPs per example and total parameter count, and their impact on model performance in MoEs, through a large-scale empirical study. We define sparsity as the ratio of inactive experts to the total number of experts, which controls the ratio of the total number of parameters to FLOPs per example in MoEs. We evaluate loss and downstream metrics for different sparsities, model sizes, and compute budgets. We find that (1) **During pretraining**, increasing a model's capacity by adding more parameters yields greater benefits than increasing FLOPs per example. We observe that the size of compute-optimal models increases as we increase the training budget (measured in terms of total FLOPs) while the active number of parameters, hence FLOPs per example, decrease for compute-optimal models and 2) **During inference**, FLOPs per example seem to play a more important role[1]. For many tasks, upstream performance is a good predictor of downstream performance and the relationship between upstream and downstream performance is not impacted by the sparsity level. However, on downstream tasks that presumably require more "reasoning", we observe that for models with the same perplexity on the pretraining data distribution, sparser models, i.e., models with fewer number of active parameters, perform worse on specific types of downstream tasks that presumably require more "reasoning".

2 The Interplay between Model Parameters and Sparsity

Is there an optimal trade-off between parameter count and FLOPs per example in MoEs under the setting where the training compute budget (i.e., total training FLOPs) is fixed?. Previous scaling law studies suggest that, conditioned on a training compute budget measured in FLOPs denoted by C, the optimal number of parameters, $N^*(C)$, exhibits a power-law

[1]A relevant discussion here is the recent trend of increasing test-time compute, e.g., OpenAI o1 model (OpenAI, 2024), achieved by generating more tokens as a way for introducing parameter-free-FLOPs.

relationship with C (Hoffmann et al., 2022). Our goal is to study how to optimally trade-off FLOPs per example and total parameters in MoEs. We use the sparsity level S that captures the balance between parameters and FLOPs per example in addition to N. Formally using notation from Appendix B, the objective can be written as:

$$(N^*, S^*) = \arg\min_{N,S} \mathcal{L}(N, S; C) \tag{1}$$

We empirically study the behavior of loss via training sparse MoEs language models ranging from 50 million to 20 billion parameters, $3e19$ to $1e21$ FLOPs and sparsity from 0% - 98% using the RedPajamaV1 (Together Computer, 2023) dataset [2]. S can be varied either by changing the number of active experts or total number of experts [3]. As the first step, considering a fixed training compute budget C, we fit a 3D surface, referred to as the IsoFLOP surface, in Figure 1a, using a polynomial function, following approach II of Hoffmann et al. (2022). We observe from Figure 1a that the IsoFLOP surface plot is parabolic along model size, suggesting that the findings of Hoffmann et al. (2022) extend to MoEs across different sparsity levels, i.e., $\mathcal{L}(N; C, S)$ is parabolic, with its optimal solution located at the inflection point. When considering the total number of parameters N, the optimal value increases as the sparsity level increases, while for the active number of parameters N_a the optimal value decreases with the sparsity level. This indicates that by increasing the sparsity level the training compute optimal models are larger but have fewer FLOPs per example, i.e., lower inference cost. Moreover, along sparsity, the pretraining loss decreases monotonically, indicating that, for the same compute budget, sparser models achieve better pretraining performance. We observe the same pattern across different training compute budgets (See Appendix F.3). To better understand and explain these observations, we study slices of the IsoFLOP surface along the axes of S and N separately as shown in Figure 5 and described in detail Appendix F.1 and Appendix F.2.

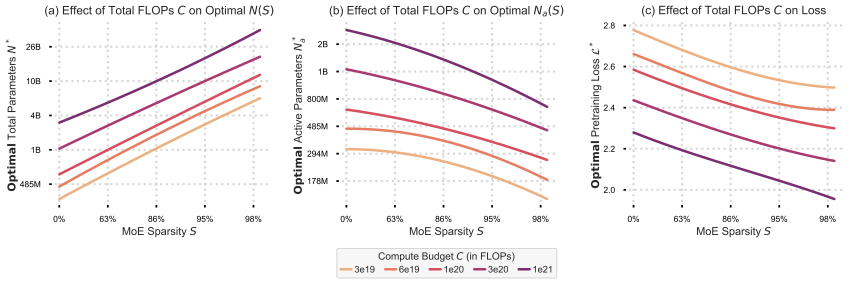

Figure 2: **Effect of compute budget on model size, number of active parameters and loss with sparsity.** Across all compute budgets, we observe that (a) the optimal model size N increases with sparsity, (b) the optimal number of active parameters N_a decreases with sparsity, and (c) the loss L decreases with sparsity.

3 Impact of Training Compute Budget on the Interaction between Model Parameters and Sparsity

Does the recipe for optimally increasing model capacity, i.e., optimal sparsity level for MoEs change as we scale up the total training compute? Figure 2 illustrates the trends for changing the total number of parameters, N^*, the number of active parameters, N_a^*, and the loss, L^*, with sparsity level across different compute budgets. Figure 2c shows that the optimal sparsity level approaches 1 across all compute budgets used in our experiments. This observation suggests that there is no diminishing effect of sparsity on the pretraining loss as we increase training compute budget, i.e., if there is no constraint on the model size, sparsity improves the performance of the model across all training budgets. In Figures 2a and 2b, , we see a consistent trend of increasing N and decreasing N_a for compute optimal models as sparsity level increases across all training compute budgets. Moreover, as can be seen in Figure 8 in Appendix F.4, when model size in terms of total number of parameters is fixed, optimal sparsity level increases with training compute budget as well as model size.

[2] A detailed description of experimental setup is provided in Appendix C

[3] See Appendix D for details.

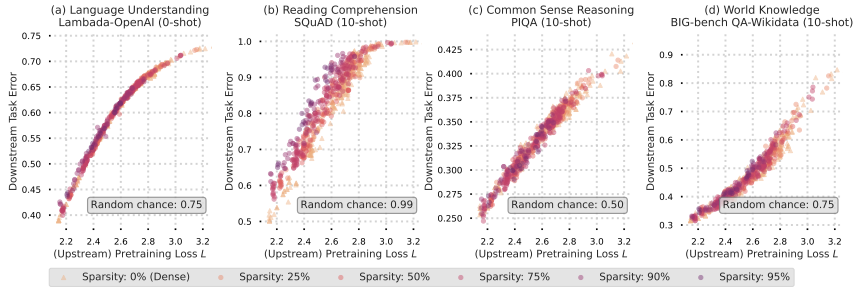

Figure 3: **Effect of sparsity on downstream vs upstream performance.** See Section 4 for detailed description.

4 Effect of MoE Sparsity on Downstream Task Performance

In this section, we study how sparsity affects the relationship between upstream and downstream performance of MoEs. We use downstream tasks from `llm-foundry`[4] evaluation suite to benchmark our pretrained models. The downstream task are divided into four pre-defined categories namely: language understanding, world knowledge, reading comprehension, and symbolic reasoning to systematically test how sparsity affects downstream versus upstream performance. We observe from Figure 3a (language understanding), Figure 3c (commonsense reasoning), and Figure 3d (world knowledge) that there is a strong correlation between upstream (pretraining) loss and downstream performance (error) across all these tasks. For these tasks, downstream performance is predictable based on upstream performance, regardless of the sparsity level. However, Figure 3b (reading comprehension) shows a task where models with higher sparsity transfer more poorly compared to denser models. This decrease in the transfer performance of sparser models on these tasks may be due to the lower inference-time compute in sparser models compared to their denser counterparts for a similar pretraining loss.

While our results may indicate that there may be no additional benefit obtained via sparsity in MoEs beyond the efficiency gains for pretraining, we caution the reader that this suggestion may be an artifact of the scale of our experiments. In the end, since, as shown in §2, sparser models are more efficient both in terms of training and inference cost (when measured in terms of theoretical FLOPs), we can reach better pretraining performance with higher sparsity levels at a lower cost, which can translate to better downstream performance.

5 Incorporating Sparsity into Scaling Laws

The scaling laws proposed by Kaplan et al. (2020) (see Appendix G.1) provide a framework for predicting loss in dense models by establishing a power-law relationship between loss L, number of parameters N and dataset size D, where N and D interact linearly. For dense transformers with a fixed total training FLOPs, C, N and D are interrelated through the equation $C = 6ND$. However, in MoEs, this relationship involves the active number of parameters N_a rather than the total parameter count N. Thus, D and N_a define the total training FLOPs rather than D and N. Furthermore, we observe from §2 that if N is fixed, the optimal sparsity level, i.e., active number of parameters would depend on N. Motivated by these observations, we suggest the following parametric form that includes a multiplicative interaction between N and S or N_a to predict the loss:

$$L(N, D, S) = \frac{a}{N^{\alpha}} + \frac{b}{D^{\beta}} + \frac{c}{(1-S)^{\lambda}} + \frac{d}{(1-S)^{\delta} N^{\gamma}} + e \tag{2}$$

The coefficients in Equation 2 are estimated using empirical data gathered from our experiments using the approach described in Appendix G. Figure 12(b) shows that the fitted law works with reasonable accuracy.

[4]Github repository: `https://github.com/mosaicml/llm-foundry`

6 Conclusion

We investigate the optimal trade-off between parameters and compute per example for maximizing model capacity. Our findings, discussed in detail in Appendix H, indicate that sparsity, as a knob that controls FLOPs per example in MoEs, is a powerful mechanism for optimizing model performance under constrained training compute budgets. By balancing the total number of parameters, compute, and sparsity, MoEs can be scaled more effectively.

Acknowledgments

The authors would like to thank Vaishaal Shankar, Fartash Faghri, Skyler Seto, Mustafa Shukor, Amitis Shidani, David Grangier, Etai Littwin, Alexander Toshev and Preetum Nakkiran for their insightful discussions, feedback and technical support that significantly contributed to the development of this paper.

References

BIG-bench authors. Beyond the imitation game: Quantifying and extrapolating the capabilities of language models. *Transactions on Machine Learning Research*, 2023. ISSN 2835-8856. URL https://openreview.net/forum?id=uyTL5Bvosj.

Sid Black, Stella Biderman, Eric Hallahan, Quentin Anthony, Leo Gao, Laurence Golding, Horace He, Connor Leahy, Kyle McDonell, Jason Phang, et al. Gpt-neox-20b: An open-source autoregressive language model. *arXiv preprint arXiv:2204.06745*, 2022.

Tom Brown, Benjamin Mann, Nick Ryder, Melanie Subbiah, Jared D Kaplan, Prafulla Dhariwal, Arvind Neelakantan, Pranav Shyam, Girish Sastry, Amanda Askell, Sandhini Agarwal, Ariel Herbert-Voss, Gretchen Krueger, Tom Henighan, Rewon Child, Aditya Ramesh, Daniel Ziegler, Jeffrey Wu, Clemens Winter, Chris Hesse, Mark Chen, Eric Sigler, Mateusz Litwin, Scott Gray, Benjamin Chess, Jack Clark, Christopher Berner, Sam McCandlish, Alec Radford, Ilya Sutskever, and Dario Amodei. Language models are few-shot learners. In H. Larochelle, M. Ranzato, R. Hadsell, M.F. Balcan, and H. Lin (eds.), *Advances in Neural Information Processing Systems*, volume 33, pp. 1877–1901. Curran Associates, Inc., 2020. URL https://proceedings.neurips.cc/paper_files/paper/2020/file/1457c0d6bfcb4967418bfb8ac142f64a-Paper.pdf.

Aidan Clark, Diego de las Casas, Aurelia Guy, Arthur Mensch, Michela Paganini, Jordan Hoffmann, Bogdan Damoc, Blake Hechtman, Trevor Cai, Sebastian Borgeaud, George van den Driessche, Eliza Rutherford, Tom Hennigan, Matthew Johnson, Katie Millican, Albin Cassirer, Chris Jones, Elena Buchatskaya, David Budden, Laurent Sifre, Simon Osindero, Oriol Vinyals, Jack Rae, Erich Elsen, Koray Kavukcuoglu, and Karen Simonyan. Unified scaling laws for routed language models. In *Proceedings of the 39th International Conference on Machine Learning*. PMLR, 2022.

R'obert Csord'as, Kazuki Irie, Jürgen Schmidhuber, Christopher Potts, and Christopher D. Manning. Moeut: Mixture-of-experts universal transformers. *ArXiv*, abs/2405.16039, 2024. URL https://api.semanticscholar.org/CorpusID:270063139.

DeepSeek-AI. Deepseek LLM: Scaling open-source language models with longtermism. *ArXiv*, abs/2401.02954, 2024. URL https://api.semanticscholar.org/CorpusID:266818336.

DeepSeek-AI. Deepseek-r1: Incentivizing reasoning capability in llms via reinforcement learning. https://github.com/deepseek-ai/DeepSeek-R1, January 2025. Accessed: 2025-01-21.

Mostafa Dehghani, Stephan Gouws, Oriol Vinyals, Jakob Uszkoreit, and Lukasz Kaiser. Universal transformers. In *International Conference on Learning Representations*, 2019. URL https://openreview.net/forum?id=HyzdRiR9Y7.

Jacob Devlin, Ming-Wei Chang, Kenton Lee, and Kristina Toutanova. BERT: Pre-training of deep bidirectional transformers for language understanding. In Jill Burstein, Christy Doran, and Thamar Solorio (eds.), *Proceedings of the 2019 Conference of the North American Chapter of the Association for Computational Linguistics: Human Language Technologies, Volume 1 (Long and Short Papers)*, pp. 4171–4186, Minneapolis, Minnesota, June 2019. Association for Computational Linguistics. doi: 10.18653/v1/N19-1423. URL https://aclanthology.org/N19-1423.

Nan Du, Yanping Huang, Andrew M. Dai, Simon Tong, Dmitry Lepikhin, Yuanzhong Xu, Maxim Krikun, Yanqi Zhou, Adams Wei Yu, Orhan Firat, Barret Zoph, Liam Fedus, Maarten Bosma, Zongwei Zhou, Tao Wang, Yu Emma Wang, Kellie Webster, Marie Pellat, Kevin Robinson, Kathleen S. Meier-Hellstern, Toju Duke, Lucas Dixon, Kun Zhang, Quoc V. Le, Yonghui Wu, Z. Chen, and Claire Cui. Glam: Efficient scaling of language models with mixture-of-experts. *ArXiv*, abs/2112.06905, 2021. URL https://api.semanticscholar.org/CorpusID:245124124.

William Fedus, Barret Zoph, and Noam Shazeer. Switch transformers: scaling to trillion parameter models with simple and efficient sparsity. *J. Mach. Learn. Res.*, 23(1), jan 2022. ISSN 1532-4435.

Elias Frantar, Carlos Riquelme Ruiz, Neil Houlsby, Dan Alistarh, and Utku Evci. Scaling laws for sparsely-connected foundation models. In *The Twelfth International Conference on Learning Representations*, 2024. URL https://openreview.net/forum?id=i9K2ZWkYIP.

Samir Yitzhak Gadre, Georgios Smyrnis, Vaishaal Shankar, Suchin Gururangan, Mitchell Wortsman, Rulin Shao, Jean Mercat, Alex Fang, Jeffrey Li, Sedrick Keh, Rui Xin, Marianna Nezhurina, Igor Vasiljevic, Jenia Jitsev, Alexandros G. Dimakis, Gabriel Ilharco, Shuran Song, Thomas Kollar, Yair Carmon, Achal Dave, Reinhard Heckel, Niklas Muennighoff, and Ludwig Schmidt. Language models scale reliably with over-training and on downstream tasks. *CoRR*, abs/2403.08540, 2024. URL https://doi.org/10.48550/arXiv.2403.08540.

Trevor Gale, Deepak Narayanan, Cliff Young, and Matei Zaharia. MegaBlocks: Efficient Sparse Training with Mixture-of-Experts. *Proceedings of Machine Learning and Systems*, 5, 2023.

Gemini Team, Rohan Anil, Sebastian Borgeaud, Yonghui Wu, Jean-Baptiste Alayrac, Jiahui Yu, Radu Soricut, Johan Schalkwyk, Andrew M Dai, Anja Hauth, et al. Gemini: A family of highly capable multimodal models, 2024. URL https://arxiv.org/abs/2312.11805.

Sachin Goyal, Ziwei Ji, Ankit Singh Rawat, Aditya Krishna Menon, Sanjiv Kumar, and Vaishnavh Nagarajan. Think before you speak: Training language models with pause tokens. In *The Twelfth International Conference on Learning Representations*, 2024. URL https://openreview.net/forum?id=ph04CRkPdC.

Xu Owen He. Mixture of a million experts. *arXiv preprint arXiv:2407.04153*, 2024.

Tom Henighan, Jared Kaplan, Mor Katz, Mark Chen, Christopher Hesse, Jacob Jackson, Heewoo Jun, Tom B. Brown, Prafulla Dhariwal, Scott Gray, Chris Hallacy, Benjamin Mann, Alec Radford, Aditya Ramesh, Nick Ryder, Daniel M. Ziegler, John Schulman, Dario Amodei, and Sam McCandlish. Scaling laws for autoregressive generative modeling. *arXiv preprint arXiv: Arxiv-2010.14701*, 2020.

Jordan Hoffmann, Sebastian Borgeaud, Arthur Mensch, Elena Buchatskaya, Trevor Cai, Eliza Rutherford, Diego de Las Casas, Lisa Anne Hendricks, Johannes Welbl, Aidan Clark, Thomas Hennigan, Eric Noland, Katherine Millican, George van den Driessche, Bogdan Damoc, Aurelia Guy, Simon Osindero, Karén Simonyan, Erich Elsen, Oriol Vinyals, Jack Rae, and Laurent Sifre. An empirical analysis of compute-optimal large language model training. In S. Koyejo, S. Mohamed, A. Agarwal, D. Belgrave, K. Cho, and A. Oh (eds.), *Advances in Neural Information Processing Systems*, volume 35, pp. 30016–30030. Curran Associates, Inc., 2022. URL https://proceedings.neurips.cc/paper_files/paper/2022/file/c1e2faff6f588870935f114ebe04a3e5-Paper-Conference.pdf.

Samy Jelassi, Clara Mohri, David Brandfonbrener, Alex Gu, Nikhil Vyas, Nikhil Anand, David Alvarez-Melis, Yuanzhi Li, Sham M Kakade, and Eran Malach. Mixture of parrots: Experts improve memorization more than reasoning. *arXiv preprint arXiv:2410.19034*, 2024.

Jared Kaplan, Sam McCandlish, Tom Henighan, Tom B. Brown, Benjamin Chess, Rewon Child, Scott Gray, Alec Radford, Jeffrey Wu, and Dario Amodei. Scaling laws for neural language models. *CoRR*, abs/2001.08361, 2020. URL https://arxiv.org/pdf/2001.08361.pdf.

Dmitry Lepikhin, HyoukJoong Lee, Yuanzhong Xu, Dehao Chen, Orhan Firat, Yanping Huang, Maxim Krikun, Noam Shazeer, and Zhifeng Chen. {GS}hard: Scaling giant models with conditional computation and automatic sharding. In *International Conference on Learning Representations*, 2021. URL https://openreview.net/forum?id=qrwe7XHTmYb.

Jan Ludziejewski, Jakub Krajewski, Kamil Adamczewski, Maciej Pióro, Michał Krutul, Szymon Antoniak, Kamil Ciebiera, Krystian Król, Tomasz Odrzygóźdź, Piotr Sankowski, Marek Cygan, and Sebastian Jaszczur. Scaling laws for fine-grained mixture of experts. In *ICLR 2024 Workshop on Mathematical and Empirical Understanding of Foundation Models*, 2024. URL https://openreview.net/forum?id=Iizr8qwH7J.

Niklas Muennighoff, Luca Soldaini, Dirk Groeneveld, Kyle Lo, Jacob Morrison, Sewon Min, Weijia Shi, Pete Walsh, Oyvind Tafjord, Nathan Lambert, Yuling Gu, Shane Arora, Akshita Bhagia, Dustin Schwenk, David Wadden, Alexander Wettig, Binyuan Hui, Tim Dettmers, Douwe Kiela, Ali Farhadi, Noah A. Smith, Pang Wei Koh, Amanpreet Singh, and Hannaneh Hajishirzi. Olmoe: Open mixture-of-experts language models, 2024. URL https://arxiv.org/abs/2409.02060.

NeMo Authors. Nemo: a toolkit for conversational ai and large language models. https://github.com/NVIDIA/NeMo, 2025.

OpenAI. Gpt-4 technical report. *PREPRINT*, 2023.

OpenAI. Openai o1 system card. *arXiv preprint arXiv: 2412.16720*, 2024.

Pranav Rajpurkar, Robin Jia, and Percy Liang. Know what you don't know: Unanswerable questions for SQuAD. In Iryna Gurevych and Yusuke Miyao (eds.), *Proceedings of the 56th Annual Meeting of the Association for Computational Linguistics (Volume 2: Short Papers)*, pp. 784–789, Melbourne, Australia, July 2018. Association for Computational Linguistics. doi: 10.18653/v1/P18-2124. URL https://aclanthology.org/P18-2124.

Siva Reddy, Danqi Chen, and Christopher D. Manning. CoQA: A conversational question answering challenge. *Transactions of the Association for Computational Linguistics*, 7:249–266, 2019. doi: 10.1162/tacl_a_00266. URL https://aclanthology.org/Q19-1016.

Noam Shazeer, *Azalia Mirhoseini, *Krzysztof Maziarz, Andy Davis, Quoc Le, Geoffrey Hinton, and Jeff Dean. Outrageously large neural networks: The sparsely-gated mixture-of-experts layer. In *International Conference on Learning Representations*, 2017. URL https://openreview.net/forum?id=B1ckMDqlg.

Together Computer. Redpajama: An open source recipe to reproduce llama training dataset. https://github.com/togethercomputer/RedPajama-Data, April 2023. Accessed: YYYY-MM-DD.

Siqi Wang, Zhengyu Chen, Bei Li, Keqing He, Min Zhang, and Jingang Wang. Scaling laws across model architectures: A comparative analysis of dense and MoE models in large language models. In Yaser Al-Onaizan, Mohit Bansal, and Yun-Nung Chen (eds.), *Proceedings of the 2024 Conference on Empirical Methods in Natural Language Processing*, pp. 5583–5595, Miami, Florida, USA, November 2024. Association for Computational Linguistics. doi: 10.18653/v1/2024.emnlp-main.319. URL https://aclanthology.org/2024.emnlp-main.319/.

Jason Wei, Yi Tay, Rishi Bommasani, Colin Raffel, Barret Zoph, Sebastian Borgeaud, Dani Yogatama, Maarten Bosma, Denny Zhou, Donald Metzler, Ed H. Chi, Tatsunori Hashimoto, Oriol Vinyals, Percy Liang, Jeff Dean, and William Fedus. Emergent abilities of large language models. *Transactions on Machine Learning Research*, 2022a. ISSN 2835-8856. URL https://openreview.net/forum?id=yzkSU5zdwD. Survey Certification.

Jason Wei, Xuezhi Wang, Dale Schuurmans, Maarten Bosma, brian ichter, Fei Xia, Ed H. Chi, Quoc V Le, and Denny Zhou. Chain of thought prompting elicits reasoning in large language models. In Alice H. Oh, Alekh Agarwal, Danielle Belgrave, and Kyunghyun Cho (eds.), *Advances in Neural Information Processing Systems*, 2022b. URL https://openreview.net/forum?id=_VjQlMeSB_J.

Mitchell Wortsman, Peter J Liu, Lechao Xiao, Katie Everett, Alex Alemi, Ben Adlam, John D Co-Reyes, Izzeddin Gur, Abhishek Kumar, Roman Novak, et al. Small-scale proxies for large-scale transformer training instabilities. *arXiv preprint arXiv:2309.14322*, 2023.

Longfei Yun, Yonghao Zhuang, Yao Fu, Eric P Xing, and Hao Zhang. Toward inference-optimal mixture-of-expert large language models. *arXiv preprint arXiv:2404.02852*, 2024.

Barret Zoph, Irwan Bello, Sameer Kumar, Nan Du, Yanping Huang, Jeff Dean, Noam Shazeer, and William Fedus. ST-MoE: designing stable and transferable sparse expert models. *arXiv preprint arXiv:2202.08906*, 2022.

Appendices

A Related Work **10**
A.1 Scaling Laws for Language Models 10
A.2 Scaling Laws for MoEs 10

B Preliminaries **12**
B.1 Mixture-of-Expert (MoE) Transformers 12

C Experimental Setup **13**

D Estimating Mixture-of-Expert (MoE) FLOPs **15**

E Related Work **17**
E.1 Scaling Laws for Language Models 17
E.2 Scaling Laws for MoEs 17

F Additional Analysis **19**
F.1 Optimal Model Size for Fixed Sparsity Level 19
F.2 Optimal Sparsity Level for Fixed Model Size 19
F.3 Interplay between parameters and FLOPs per example 20
F.4 Effect of training budget and model size on optimal MoE sparsity 20
F.5 Effect of sparsity on downstream task performance 22
F.6 Comparing IsoFLOP Surface Analysis with Independent 2d IsoFLOPs . 23

G Incorporating Sparsity into Scaling Laws **26**
G.1 Scaling Law for Dense Models 26
G.2 Fitting Coefficients to Scaling Laws for Sparsity 26
G.3 Hyperparameters and Estimated Coefficients 26

H Discussion **28**

I Conclusion **29**

J Limitations **30**

A Related Work

MoEs (Shazeer et al., 2017; Lepikhin et al., 2021; Fedus et al., 2022; DeepSeek-AI, 2025) have become a prominent architecture in language modeling due to their ability to decouple computational cost from parameter count. This characteristic necessitates scaling laws that accurately account for both parameters and FLOPs per token. In the following, we discuss scaling laws studies for language models followed followed by existing scaling law studies for MoEs.

A.1 Scaling Laws for Language Models

Scaling laws have proven to be a powerful framework for understanding and predicting the performance of language models. Existing studies, such as Kaplan et al. (2020) and Hoffmann et al. (2022), reveal that power-law relationships govern model performance as a function of factors like model size, data size, and compute budget, offering predictable performance improvements with increased resources.

Hoffmann et al. (2022) emphasizes the critical balance between model size and the number of training tokens when the training compute budget is fixed, showing that scaling the model without corresponding data increases can lead to suboptimal performance. Additionally, DeepSeek-AI (2024) explores more nuanced scaling behaviors by incorporating data quality, demonstrating that higher-quality data allows for more efficient scaling, and thus, a larger portion of the compute budget should be allocated to increasing model size.

Recent work extends scaling law analysis to specialized contexts, including over-training (Gadre et al., 2024), downstream task performance, and multilingual or multi-modal settings, where scaling laws provide valuable insights and can be adapted to address specific challenges.

A.2 Scaling Laws for MoEs

Mixture-of-Experts (MoE) models (Shazeer et al., 2017; Lepikhin et al., 2021; Fedus et al., 2022; DeepSeek-AI, 2025) have emerged as a powerful architecture for language modeling, primarily because they decouple computational cost from parameter count. This separation between parameters and FLOPs per token in MoE architectures calls for scaling laws that can accurately factor in the contributions of both.

Previous research on the scaling behavior of MoE models has established foundational scaling laws, incorporating factors such as total parameter count, the number of experts, and the granularity of these experts (Clark et al., 2022; Ludziejewski et al., 2024; Wang et al., 2024). However, these studies typically assume a fixed configuration for other critical variables influencing FLOPs per token, such as the number of active experts per input. In contrast, we propose a generalized scaling law that considers variables like active parameter count and sparsity level, thereby expanding the applicability of MoE scaling laws.

A common theme in the literature suggests that training sparser models—achieved by increasing the number of smaller experts—offers significant gains in efficiency for both pre-training and inference phases. Through a comprehensive large-scale study, we provide empirical evidence for this, analyzing the impact of sparsity level on efficiency and defining optimal configurations.

Supporting this, Du et al. (2021) demonstrates GLaM's superior efficiency and performance compared to GPT-3, showing that MoE architectures can achieve high performance with significantly lower computational and energy costs. Further insights are offered by Clark et al. (2022), who analyze scaling behaviors across various MoE routing techniques. While their study finds that MoEs generally outperform dense models, it also notes diminishing benefits as base model sizes grow. Ludziejewski et al. (2024) challenge this conclusion, attributing the diminished returns partly to the fixed number of training tokens across models and constant expert sizes. By introducing "granularity" and adjusting training durations, they demonstrate that MoEs can outperform dense models across any compute budget, debunking the notion of diminishing returns for MoEs with adaptive expert configurations. More

recently, Jelassi et al. (2024) finds that, on downstream tasks, MoEs scale efficiently with the number of experts (i.e., increasing sparsity) on memorization tasks, but their reasoning capabilities saturate and lag behind dense models on tasks requiring complex reasoning when compared based on total number of parameters.

Another approach by He (2024) explores the benefits of training MoEs with larger numbers of smaller experts rather than the conventional setup of fewer, larger experts. They introduce Parameter Efficient Expert Retrieval (PEER), a novel routing mechanism designed to tackle the computational and optimization challenges that arise when handling a high number of experts, thus enabling efficient scaling of MoE models.

Lastly, Yun et al. (2024) draws attention to the increased inference costs associated with scaling MoEs by adding experts. While additional experts may not substantially affect training costs, they can inflate inference costs, thereby diminishing deployment efficiency. To address this, the study proposes an over-trained budget allocation strategy, optimizing MoE models for both performance and efficiency in deployment.

B Preliminaries

In this section, we provide a brief overview of Mixture-of-Expert (MoE) Transformers.

B.1 Mixture-of-Expert (MoE) Transformers

Mixture-of-Experts Transformers modify the standard transformer architecture by introducing in the MLP layer. In this design, the experts are MLP (Multi-Layer Perceptron) modules that follow the attention mechanism and are selectively activated for each token. A gating mechanism determines which MLP experts are most relevant for each token, ensuring that only a subset of experts (top-k) is active at any given time, while the rest remain inactive. Below, we provide the notations used throughout the paper for various terms related to training MoEs.

Total and Active Parameters: In MoEs, we distinguish between total and active parameters, denoted by N and N_a, respectively. The total parameter count, N, includes all parameters of the network, encompassing both the experts and the rest of the architecture. The active parameter count, N_a, refers to the parameters associated with the active portion of the experts, along with the rest of the network that is always utilized.

Top-k Expert Selection: In MoEs, the gating mechanism assigns tokens to a subset of experts using a top-k selection process, where k denotes the number of experts activated for each token. The gate computes a relevance score for each expert, and the top k experts with the highest scores are selected and activated. This selective activation limits the computational overhead by ensuring that only a fraction of the experts are used per token.

Expansion Factor and Granularity: The expansion factor, typically denoted by E, represents the increase in model capacity due to the inclusion of multiple experts, measured as a multiplicative factor relative to the base dense model. The granularity, G, determines the size of each expert relative to the size of the MLP module in the base dense model. The total number of experts in the model is given by $E \times G$, where E scales the capacity and G controls the level of granularity.

Sparsity (S): In general, sparsity is defined as the ratio of inactive to total parameters. However, in the context of MoEs, we focus on the sparsity of the MLP modules specifically. Therefore, we define the sparsity level as the ratio of inactive to total experts, given by:

$$S = \frac{\text{number of non-active experts}}{\text{number of total experts}}. \tag{3}$$

This definition provides an interpretable measure of sparsity but cannot be directly used to calculate the active parameter count N_a due to the contribution of other parameters in the model that remain unsparsified.

C Experimental Setup

We train and evaluate auto-regressive sparse Mixture-of-Experts (MoE) language models of varying sizes and configurations on subsets of the RedPajamaV1 dataset Together Computer (2023). The key variables we explore in our experiments are total model parameters N, training compute budget C, and the MoE sparsity S.

Pre-training data. Our models are pre-trained on subsets of the RedPajamaV1 dataset[5] Together Computer (2023), which attempts to replicate the LLaMA pre-training data recipe and comprises 1.2 trillion tokens from sources such as Common Crawl, C4, GitHub, and Wikipedia. In all our experiments, the effective dataset size is adjusted based on the training compute budget C and the model size N. We tokenize the data using the GPT-NeoX tokenizer Black et al. (2022), which has a vocabulary size of $50,432$ tokens.

Model and tokenizer. We use auto-regressive transformer-based MoE language models in order to study compute-parameter trade-offs by varying MoE sparsity. We use the Megablocks library Gale et al. (2023) to train dropless MoEs in which the routing mechanism ensures that all tokens are efficiently routed without being dropped due to routing capacity constraints.

Optimizer and scheduler. We optimize our models using the scale-free Adam optimizer[6] with variable learning rate, a weight decay of 1×10^{-5}, and fixed Adam-specific parameters $\beta = (0.9, 0.95)$ and $\varepsilon = 1 \times 10^{-8}$. We use a learning rate scheduler consisting of a linear warm-up phase followed by a cosine decay. The warm-up phase increases the learning rate from 0 to the base learning rate over a fraction of the total training steps (selected from $\{0.1, 0.05, 0.02\}$). After warm-up, the learning rate decays following a cosine schedule for the remaining training steps.

Fitting IsoFLOP surfaces. Recall that in Section 2, we fit isoFLOP surfaces to predict pretraining loss L as a polynomial function of model size N and MoE sparsity S for a fixed training budget C. The polynomial function takes the form

$$L(N, S) = \sum_{i=1}^{\alpha_1} a_i \hat{N}^i + \sum_{i=1}^{\alpha_2} b_i \hat{S}^i + \sum_{i=1}^{\alpha_3} c_i (\hat{N} \cdot \hat{S})^i + d \tag{4}$$

where $\hat{N} = \log N$ and $\hat{S} = -\log(1-S)$—we find that applying log transformations improves the fit of the resulting IsoFLOP surface. Through a grid search over the polynomial coefficients $\alpha_1, \alpha_2, \alpha_3 \in \{0, 1, 2, 3, 4\}$, we found that the best fit was obtained for $\alpha = \beta = \gamma = 2$, i.e., a quadratic polynomial over $\hat{N}$ and $\hat{S}$. We evaluate the fitted IsoFLOP surfaces in Figure 1 by (a) re-running the fitting procedure $k = 100$ times on randomly subsampled data and (b) evaluating the Pearson correlation between the true and predicted pretraining loss values on a set of held-out data points.

Hyperparameters. We fix a subset of hyperparameters for which changing values in preliminary experiments (a) did not significantly improve pre-training loss, (b) the optimal value remained the same across several model configurations, or (c) in order to reduce the search space (i.e., limited compute resources). Specifically, we first opted to use z-router loss Zoph et al. (2022) and qk-normalization Wortsman et al. (2023) in order to stabilize training for large MoEs. Second, we fixed MoE router jitter noise to 0, as it did not improve performance. We also fixed our batch size to 1024 for all model sizes.

We swept over hyperparameters that, when adjusted, (a) significantly improved pre-training loss and (b) the optimal values varied across different model configurations. We increase the MoE sparsity by decreasing the number of active experts and/or increasing the number of total experts. We also varied the MoE granularity Ludziejewski et al. (2024), MoE load

[5]GitHub repository: `https://github.com/togethercomputer/RedPajama-Data`

[6]Scale-free Adam: `https://fabian-sp.github.io/posts/2024/02/decoupling/`

balancing regularizer, Adam learning rate, and linear warm-up steps (fraction) in order to improve pre-training loss. The table below summarizes our hyperparameter sweeps:

Table 1: Hyperparameter configurations and search spaces

Hyperparameter	**Configuration**	**Search Space**
Sparsity Level	Tuned	$\{0, 25, 50, 75, 90, 95, 98\}\%$
Number of Total Experts	Tuned	Adjusted depending on sparsity
Number of Active Experts	Tuned	Adjusted depending on sparsity
Granularity	Tuned	$\{1, 2\}$
Learning Rate	Tuned	$[0.003, 0.002, 0.001]$
Load Balancing Factor	Tuned	$\{0.02, 0.05\}$
Warm-up Steps	Tuned	$\{2, 5, 10\}\%$
Batch Size	Constant	1024
Jitter Noise	Constant	0
z-Loss	Constant	0
z-Router Loss	Constant	0.001
QK Norm	Constant	Applied

It is also noteworthy that, in this paper, we have prioritized training compute-optimal models, in contrast to many published results on large language models (LLMs), which often rely on over-trained models. As a result, the performance of the models we use for the analysis in this paper is not directly comparable to those of other studies, where they overtrain smaller language models, to reduce the cost of inference relative to training.

D Estimating Mixture-of-Expert (MoE) FLOPs

Similar to prior work on scaling laws (e.g., Kaplan et al. (2020); Hoffmann et al. (2022); Ludziejewski et al. (2024)), we use theoretical FLOP estimates as proxies for training and inference costs of language models. In this section, we (a) outline our methodology for estimating FLOPs for MoEs and (b) show that the proposed estimator closely approximates empirical FLOPs of large-scale MoEs.

Setup and notation. Consider an MoE model with n_{layers} MoE layers, each with an embedding dimension of d_{model}. We denote the number of total experts and active experts in each MoE layer by E_{total} and E_{active} respectively. Following Ludziejewski et al. (2024), we let G denote the MoE granularity, which defaults to 1 and controls the size of each expert relative to the size of a feed-forward layer in an equivalent dense transformer. In order to change sparsity in a more granular manner, we treat the number of active experts as an independent variable that does not scale with granularity G. In our experiments, we use a vocabulary size $n_{\text{vocab}} = 50,432$, a context length n_{ctx} of 2048, and GLU modules (Gated Linear Units) (Shazeer et al., 2017) over feed-forward modules as the architecture of choice for MoE experts. We also set the (a) hidden dimension of each GLU expert d_{ffn} to $4 \cdot d_{\text{model}}$ and (b) instantiate MoEs where the number of attention heads n_{heads} times the dimensionality for each head d_{head} equals d_{model}, i.e., $n_{\text{heads}} d_{\text{head}} = d_{\text{model}}$.

Estimating module-specific FLOPs. To estimate the FLOPs of a given MoE model, we first individually estimate the FLOPs per token incurred by a forward *and* backward pass through every module in MoEs. Then, we aggregate these estimates to obtain the final estimator for the FLOPs per token incurred by a forward *and* backward pass through the model.

Like in prior work on scaling laws (Kaplan et al., 2020; Hoffmann et al., 2022), we take a two-step approach to estimate module-specific FLOPs. Given a module, we first estimate the number of parameters in the module and then scale this with an appropriate constant corresponding to the number of add-multiply operations per parameter through a forward and backward pass of the given module. We also omit non-leading terms such as non-linearities, biases, and layer normalization in our estimation. We estimate the FLOPs per token for attention modules, MoE routers, MoE experts, and the final un-embedding layer as follows:

1. **Attention module.** We estimate the FLOPs incurred via the QKV (and final) projections, attention logits, and attention values of all heads in a multi-head attention module as follows.
   - *QKV (and final) projections.* These projections involve $4 \cdot d_{\text{model}} n_{\text{heads}} d_{\text{heads}} = 4 d_{\text{model}}^2$ parameters. Following Kaplan et al. (2020), we use the multiplicative constant $C = 6$ to account for the add-multiply operations per parameter in a forward and backward pass through linear modules, resulting in a FLOPs-per-token estimate of $4 \cdot C \cdot d_{\text{model}}^2$.
   - *Attention logits.* The FLOPs required to compute the attention logits for all n_{ctx} tokens equals $C \cdot n_{\text{ctx}}^2 d_{\text{model}}$ FLOPs, making the FLOP-per-token estimate equal to $C \cdot n_{\text{ctx}} d_{\text{model}}$.
   - *Attention values.* The computation of attention values requires a per-token weighted sum over n_{ctx} d_{model}-dimensional vectors, making the estimate $C \cdot n_{\text{ctx}} d_{\text{model}}$.
2. **MoE module.** Given an MoE layer, we estimate the FLOPs incurred by its router and all experts separately.
   - *Router.* The MoE routing linearly maps a d_{model}-dimensional token embedding to a E_{total}-dimensional logit vector, which is subsequently used to map the token to E_{active} active experts. Following Ludziejewski et al. (2024), we use a multiplicative constant $R = 14$ that accounts for the add-multiply-route operations per router parameter. The resulting FLOP estimate equals $R \cdot d_{\text{model}} E_{\text{total}}$

- *Experts.* Each MoE experts corresponds to a GLU module (Shazeer et al., 2017) with $d_{\text{ffn}} = 4 \cdot d_{\text{model}}$. Since there are E_{active} active experts with granularity G, each involving three linear projections, this results in a FLOP estimate of ${}^{1}/_{G} \cdot 3 \cdot E_{\text{active}} \cdot C \cdot d_{\text{model}} d_{\text{ffn}} = {}^{12C}/_{G} \cdot E_{\text{active}} \cdot d_{\text{model}}^2$.

3. **Un-embedding layer.** The un-embedding linear layer maps the final d_{model}-dimensional embedding of a token to n_{vocab}-dimensional logits, making the FLOPs-per-token $C \cdot n_{\text{vocab}} d_{\text{model}}$.

Estimating MoE FLOPs. We can aggregate the module-level FLOP estimates described above to estimate the FLOPs per token required for a single forward and backward pass through a given MoE model as follows:

$$n_{\text{layer}}\left(4Cd_{\text{model}}^2 + 2Cd_{\text{model}}n_{\text{ctx}} + {}^{12C}/_{G}E_{\text{active}}d_{\text{model}}^2 + Rd_{\text{model}}E_{\text{total}}\right) + Cn_{\text{vocab}}d_{\text{model}}$$

When ${}^{E_{\text{total}}}/_{d_{\text{model}}}$ is small, which is typically the case in practice, the FLOPs induced by MoE routing can be ignored as they contribute negligibly to the estimator. This allows us to simplify the estimator to:

$$\text{MoE FLOPs per token} := C \cdot n_{\text{layers}} d_{\text{model}}^2 \left(4 + \frac{2n_{\text{ctx}}}{d_{\text{model}}} + \frac{12E_{\text{active}}}{G} + \frac{n_{\text{vocab}}}{d_{\text{model}} n_{\text{layers}}}\right) \quad (5)$$

Evaluating $6N_aD$ as a FLOPs-per-token estimator in MoE Models For standard dense transformers, the FLOPs are often estimated as $6ND$ (Kaplan et al., 2020; Hoffmann et al., 2022). Given that D is fixed and not adjusted dynamically, N can serve as a relative estimator of FLOPs per token for dense transformer models.

To adapt the $6ND$ estimator for MoE models, we replace N with N_a (the active number of parameters)—the number of parameters used in every forward and backward pass. In Figure 4, we evaluate the accuracy of the $6N_aD$ estimator by plotting the ratio between the MoE FLOPs estimator described in Equation 5 and $6N_aD$ as a function of model size N and a fixed context length $D = 2048$. The results show that, across all sparsity levels, the ratio remains close to one, and the gap between the two estimators decreases as model size N increases.

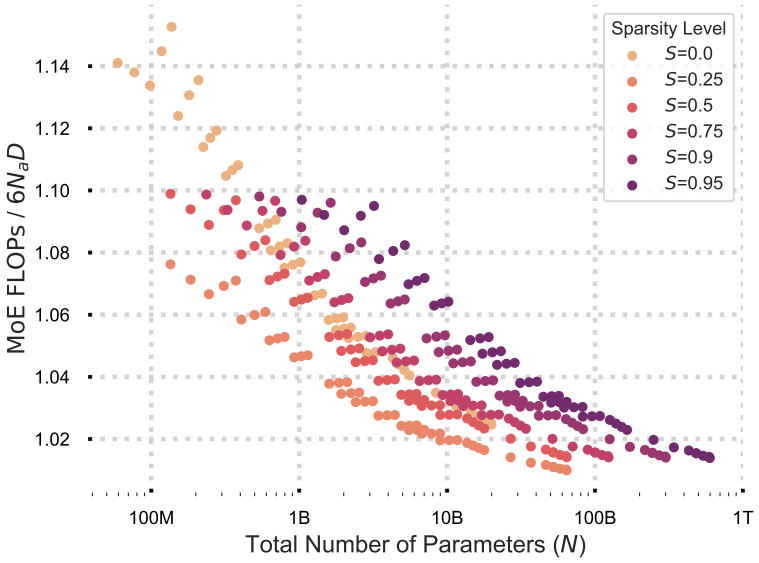

Figure 4: **Accuracy of $6N_aD$ FLOPs Estimator for MoEs**. Ratio of the MoE FLOPs estimator (Equation 5) to the $6N_aD$ estimator as a function of the total number of parameters, for a fixed context length of $D = 2048$, used in our experiments.

E Related Work

MoEs (Shazeer et al., 2017; Lepikhin et al., 2021; Fedus et al., 2022; DeepSeek-AI, 2025) have become a prominent architecture in language modeling due to their ability to decouple computational cost from parameter count. This characteristic necessitates scaling laws that accurately account for both parameters and FLOPs per token. In the following, we discuss scaling laws studies for language models followed followed by existing scaling law studies for MoEs.

E.1 Scaling Laws for Language Models

Scaling laws have proven to be a powerful framework for understanding and predicting the performance of language models. Existing studies, such as Kaplan et al. (2020) and Hoffmann et al. (2022), reveal that power-law relationships govern model performance as a function of factors like model size, data size, and compute budget, offering predictable performance improvements with increased resources.

Hoffmann et al. (2022) emphasizes the critical balance between model size and the number of training tokens when the training compute budget is fixed, showing that scaling the model without corresponding data increases can lead to suboptimal performance. Additionally, DeepSeek-AI (2024) explores more nuanced scaling behaviors by incorporating data quality, demonstrating that higher-quality data allows for more efficient scaling, and thus, a larger portion of the compute budget should be allocated to increasing model size.

Recent work extends scaling law analysis to specialized contexts, including over-training (Gadre et al., 2024), downstream task performance, and multilingual or multi-modal settings, where scaling laws provide valuable insights and can be adapted to address specific challenges.

E.2 Scaling Laws for MoEs

Mixture-of-Experts (MoE) models (Shazeer et al., 2017; Lepikhin et al., 2021; Fedus et al., 2022; DeepSeek-AI, 2025) have emerged as a powerful architecture for language modeling, primarily because they decouple computational cost from parameter count. This separation between parameters and FLOPs per token in MoE architectures calls for scaling laws that can accurately factor in the contributions of both.

Previous research on the scaling behavior of MoE models has established foundational scaling laws, incorporating factors such as total parameter count, the number of experts, and the granularity of these experts (Clark et al., 2022; Ludziejewski et al., 2024; Wang et al., 2024). However, these studies typically assume a fixed configuration for other critical variables influencing FLOPs per token, such as the number of active experts per input. In contrast, we propose a generalized scaling law that considers variables like active parameter count and sparsity level, thereby expanding the applicability of MoE scaling laws.

A common theme in the literature suggests that training sparser models—achieved by increasing the number of smaller experts—offers significant gains in efficiency for both pre-training and inference phases. Through a comprehensive large-scale study, we provide empirical evidence for this, analyzing the impact of sparsity level on efficiency and defining optimal configurations.

Supporting this, Du et al. (2021) demonstrates GLaM's superior efficiency and performance compared to GPT-3, showing that MoE architectures can achieve high performance with significantly lower computational and energy costs. Further insights are offered by Clark et al. (2022), who analyze scaling behaviors across various MoE routing techniques. While their study finds that MoEs generally outperform dense models, it also notes diminishing benefits as base model sizes grow. Ludziejewski et al. (2024) challenge this conclusion, attributing the diminished returns partly to the fixed number of training tokens across models and constant expert sizes. By introducing "granularity" and adjusting training durations, they demonstrate that MoEs can outperform dense models across any compute budget, debunking the notion of diminishing returns for MoEs with adaptive expert configurations. More

recently, Jelassi et al. (2024) finds that, on downstream tasks, MoEs scale efficiently with the number of experts (i.e., increasing sparsity) on memorization tasks, but their reasoning capabilities saturate and lag behind dense models on tasks requiring complex reasoning when compared based on total number of parameters.

Another approach by He (2024) explores the benefits of training MoEs with larger numbers of smaller experts rather than the conventional setup of fewer, larger experts. They introduce Parameter Efficient Expert Retrieval (PEER), a novel routing mechanism designed to tackle the computational and optimization challenges that arise when handling a high number of experts, thus enabling efficient scaling of MoE models.

Lastly, Yun et al. (2024) draws attention to the increased inference costs associated with scaling MoEs by adding experts. While additional experts may not substantially affect training costs, they can inflate inference costs, thereby diminishing deployment efficiency. To address this, the study proposes an over-trained budget allocation strategy, optimizing MoE models for both performance and efficiency in deployment.

F Additional Analysis

F.1 Optimal Model Size for Fixed Sparsity Level

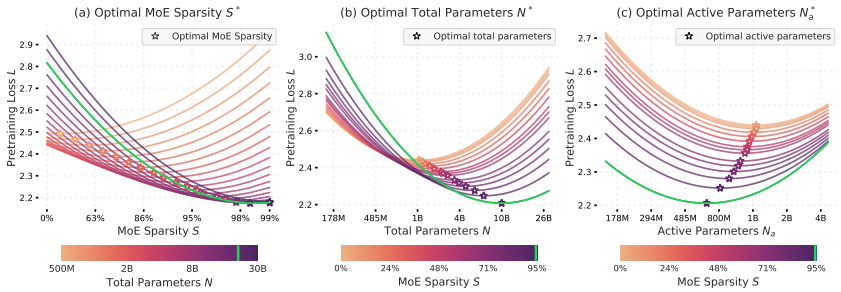

Figure 5: **IsoFLOP slices along Sparsity and Model Size ($C = 1e20$).** We use fitted isoFLOP surfaces (Section 2) to analyze how sparsity **S** and model size **N** impact the loss **L** for a fixed compute budget. We identify optimal points by (a) fixing **N** and varying **S**, (b) fixing **S** and varying **N** and (c) fixing **S** and varying active parameters $\mathbf{N_a}$. Observe that (a) the optimal sparsity S increases with increasing model size N and converges to 1 while (b) and (c) show that the optimal model size N and active parameter count N_a increase and decrease respectively with increasing sparsity levels. (see Figure 7 in Appendix F.3 for other total training compute budgets.)

To simplify the problem of understanding the joint role of N and S in predicting the loss L, we break the problem, Equation 1, into two parts. In this appendix we examine the following question:

- *"How does el impact the scaling laws of the relationship between N and C for training-compute optimal models?"* To address this question in §F.1, we fix S and vary N, studying how optimal N and N_a change for different values of S:

$$N^* = \arg\min_N \mathcal{L}(N; C, S) \tag{6}$$

Here we examine how sparsity influences scaling laws governing the relationship between N, N_a and C for training-compute optimal models, i.e. how does N^* and N_a^*, for a given C, S (Equation 6), change as we increase S? Looking at slices of the IsoFLOP surface along the model size dimension, in Figure 5b and Figure 5c, we observe how the IsoFLOP curves shift along loss and model size. Considering the training-compute optimal model, for a fixed compute budget, loss decreases as we increase sparsity. Furthermore, while sparser models have larger N compared to denser models, as seen in Figure 5b, they have a smaller active parameter count N_a; hence, fewer FLOPs per example. Intuitively, more parameters in total increase the capacity of the sparser models to fit the data, while fewer number of active parametes, hence fewer FLOPs per example, allow the model to be trained with more tokens, i.e., higher D, for the same training compute budget.

F.2 Optimal Sparsity Level for Fixed Model Size

In this section we aim to understand the dynamics between the total number of parameters and FLOPs per example in MoEs. Specifically, we consider the following question:

- *"Is there an optimal balance between total number of parameters and the sparsity level under fixed training-compute budget?"* To address this question in §F.2, we fix N and vary S, studying how optimal S changes across different values of N:

$$S^* = \arg\min_S \mathcal{L}(S; C, N) \tag{7}$$

In Appendix F.1 we are considering the case where there is no bound on the total number of parameters. In this case, we observe that under fixed training compute budget in terms of FLOPs, it is better to train sparser models with higher total number of parameters.

However in practical scenarios it is reasonable to assume that there would be some bounds on the memory and hence the total number of parameters of a model. This leads us to a fundamental question: Is there an optimal balance between the total number of parameters and and FLOPs per example under a fixed training-compute budget? Thus, we investigate the optimal sparsity level when total number of parameters is fixed. Specifically, we ask: Given N and C, How does S^* change as we vary N?

To address this, we look into slices of the IsoFLOP surface along the sparsity dimension. As we see in Figure 5a, for a fixed training compute budget and fixed model size $\mathcal{L}(S; N, C)$ exhibits a parabolic profile, reaching its optimum value at the vertex where $S = S^*$. It is noteworthy that for a given total training compute, there is threshold value N_{th} for the total number of parameters, where for larger models, models with $N > N_{th}$, increasing sparsity always has a positive impact, i.e., optimal sparsity level approaches 1.0. More accurately, for a fixed compute budget the optimal sparsity level increases with model size and converges to 1 as the model size grows (see Figure 8 in §F.4 in the Appendix for more details). Note that the optimal model, here is not the largest model, i.e., there is a compute optimal model size in terms of total parameters even after sparsity is introduced, and increasing total number of parameters leads to under-training if training compute budget is fixed.

These results highlight the importance of balancing the number of parameters with FLOPs per example in MoEs. Intuitively, when the total number of parameters is small, higher sparsity results in fewer active parameters, and thus fewer FLOPs per example. This reduction in FLOPs per example may lead to inefficiencies during both training and inference. Conversely, when the total number of parameters is large, for a reasonable amount of FLOPs per example, a fixed compute budget may not allow sufficient training on enough tokens to make use of the model's additional capacity.

F.3 Interplay between parameters and FLOPs per example

IsoFLOP surface: Compared to Hoffmann et al. (2022) we include the sparsity variable and fit a single 3d IsoFLOP surface across all data points, rather than fitting separate 2d IsoFLOP curves for fixed sparsity levels or model sizes. We conducted a grid search to determine the optimal polynomial degree for N, S, and the interaction term $N \times S$, finding that a degree of $(2, 2, 2)$ resulted in the lowest cross-validation error. Both N and S are in log space.

Recall that in Section 2, we showed that isoFLOP curves were predictive of pretraining loss for different parameter counts and sparsity levels. In this section, we show similar results with additional training compute budgets.

1. In Figure 6, we first show that IsoFLOP surfaces mapping model size N and sparsity level S to pre-training loss L are predictive in a similar way for all training compute budgets that we consider, ranging from 3e19 to 1e21 FLOPs.
2. In Figure 7, we analyze the fitted IsoFLOP surfaces (one for each training budget) and find that the (a) effect of model size N on optimal MoE sparsity S^* and (b) the effect of MoE sparsity S on the optimal total and active parameters, $N*$ and N^*_a, is similar for all training budgets.

F.4 Effect of training budget and model size on optimal MoE sparsity

Recall that in Section 3, we demonstrated how the relationship between optimal total parameters $N*$, optimal active parameters $N*_a$, and optimal pretraining loss L predictably changes as a function of sparsity S and training budget C. In this section, we use the fitted isoFLOP surfaces to analyze how the optimal MoE sparsity S^* changes as a function of total parameters N and training budget C, as shown in Figure 8. Our main findings are:

- Across all training budgets (ranging from 3e19 to 1e21 FLOPs), increasing the total parameters N leads to an increase in the optimal sparsity level S^*.
- For a fixed model size (i.e., total parameters N), increasing the training budget C generally reduces the optimal sparsity level S^*.

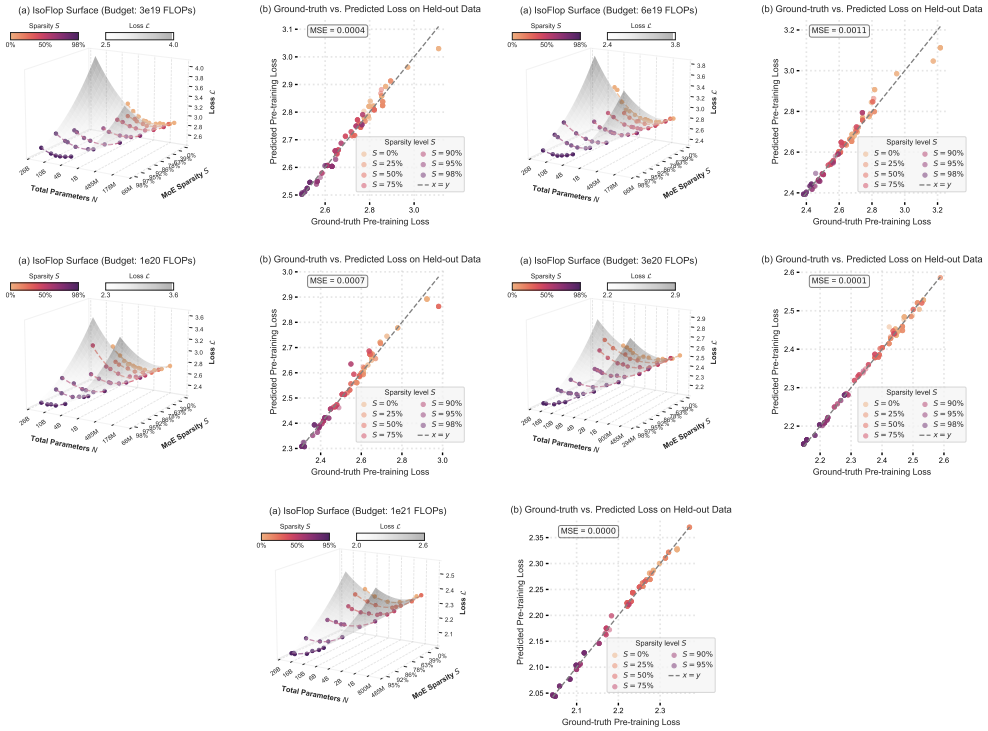

Figure 6: **IsoFLOP surfaces over total parameters N, MoE sparsity S, and pretraining loss L for different compute budgets**. The rows correspond to IsoFLOP surface fitted using models trained with a budget of 3e19, 6e19, 1e20, 3e20, and 1e21. The subplots on the left visualize IsoFLOP surfaces mapping total parameters N and sparsity level S to pretraining loss L. The subplots on the right correlate the ground-truth pretraining loss with the estimated pretraining loss on held-out data. Taken together, these results show that isoFLOP surfaces are accurate proxies for understanding how model size and MoE sparsity jointly impact pretraining loss.

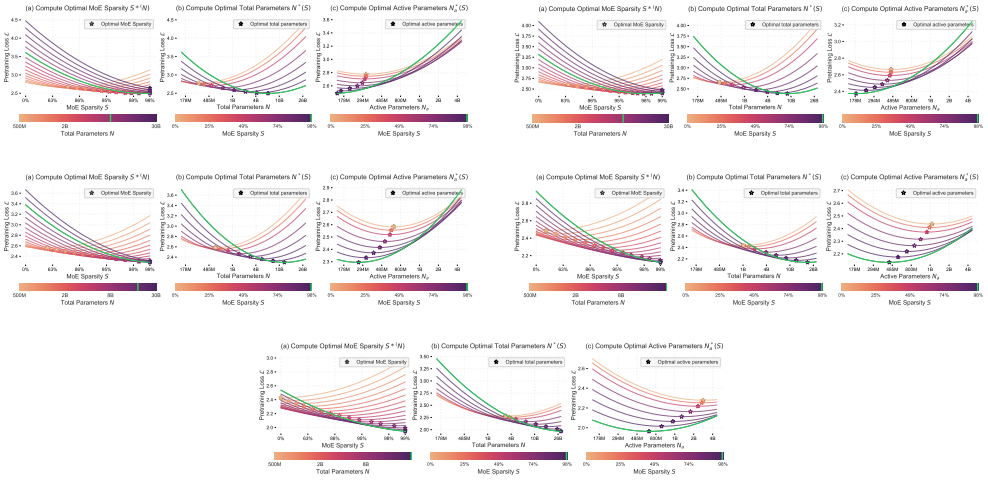

Figure 7: **Optimal MoE configurations predictably change with training compute budget.** Each row corresponds to an analysis of how optimal MoE sparsity S^*, total parameters N^*, and active parameters N_a^* change for a given training budget. The subplots on the left show that (a) increasing the training budget increases the model size N (denoted with black dots) with the minimum pretraining loss and (b) for models smaller than a threshold (which increases with training budget), dense models (i.e., 0% sparsity) fare better than sparse MoEs. The subplots in the second and third panel show that (a) increasing MoE sparsity increases the optimal total parameters N^* and decreases the optimal active parameters N_a^*. In both cases, for a fixed sparsity level, increasing the budget shifts increases the optimal total and active parameters.

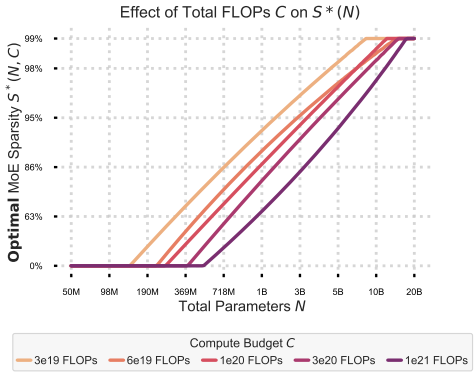

Figure 8: **Effect of training budget C and total parameters N on sparsity.** Optimal sparsity S^* changes with respect to the total number of parameters N and the training budget C. The x-axis represents the total parameters N on a logarithmic scale, and the y-axis shows the optimal sparsity S^*.

- The relationship between model size N and optimal $S*$ is not linear. For smaller models (up to about $500 \cdot 10^6$ parameters), the optimal sparsity remains at 0 (i.e., dense) for most compute budgets.

F.5 Effect of sparsity on downstream task performance

In Section 4, we analyzed the relationship between upstream pre-training loss and downstream task performance across different MoE sparsity levels. We found that language understanding and world knowledge tasks generally showed a strong correlation between upstream and downstream performance, while reading comprehension tasks seemed to favor denser models to some extent.

In this section, we provide additional plots for a broader range of tasks within each category to further support our findings. We consider the following tasks:

- **Common Sense Reasoning**: PIQA, CommonSenseQA, OpenBookQA, COPA
- **Language Understanding**: LAMBADA, HellaSwag, Winograd, Winogrande
- **Reading Comprehension**: SQuAD, CoQA, BoolQ
- **World Knowledge**: TruthfulQA, ARC-Easy, ARC-Challenge

Figure 9 shows the relationship between upstream pre-training loss and downstream task performance for these additional tasks. Each row corresponds to a task category and each subplot represents a different task, with points colored according to MoE sparsity S. The x-axis represents the upstream pre-training loss, while the y-axis shows the downstream task performance metric (usually accuracy or error rate). These results supplement our main findings from Section 4:

- We observe consistent trends across tasks within each category, with language understanding and world knowledge tasks showing strong correlations between upstream and downstream performance regardless of sparsity.
- Reading comprehension tasks continue to show a slight advantage for denser models, while common sense reasoning tasks (which can be considered part of the symbolic problem-solving category) show more varied relationships between upstream and downstream performance.

F.6 Comparing IsoFLOP Surface Analysis with Independent 2d IsoFLOPs

Recall that in Section 2, we used IsoFLOP surfaces that predict pre-training loss across varying parameter counts and sparsity levels to understand how optimal sparsity and optimal model size depend on each other.

In this section, we evaluate whether these findings remain consistent when we do not rely on fitted IsoFLOP surfaces. Specifically, similar to Approach II in Hoffmann et al. (2022), we directly fit univariate quadratic functions that map model size N to pre-training loss L, independently for each sparsity level and training compute budget. We then assess these univariate fits to determine whether our findings in Section 2 hold.

- In Figure 11, each row shows how the optimal total and active parameters change as a function of MoE sparsity for fixed training budgets. As in our findings from Section 2 (Figure 5), increasing sparsity increases the optimal total parameters while decreasing the optimal active parameters. Moreover, larger compute budgets still result in higher optimal total and active parameters, regardless of the sparsity level.
- Furthermore, in Figure 10, we observe that across all training compute budgets, increasing sparsity reduces the optimal pre-training loss. This is consistent with the trends identified in Section 3 (Figure 2), thereby validating our earlier results.

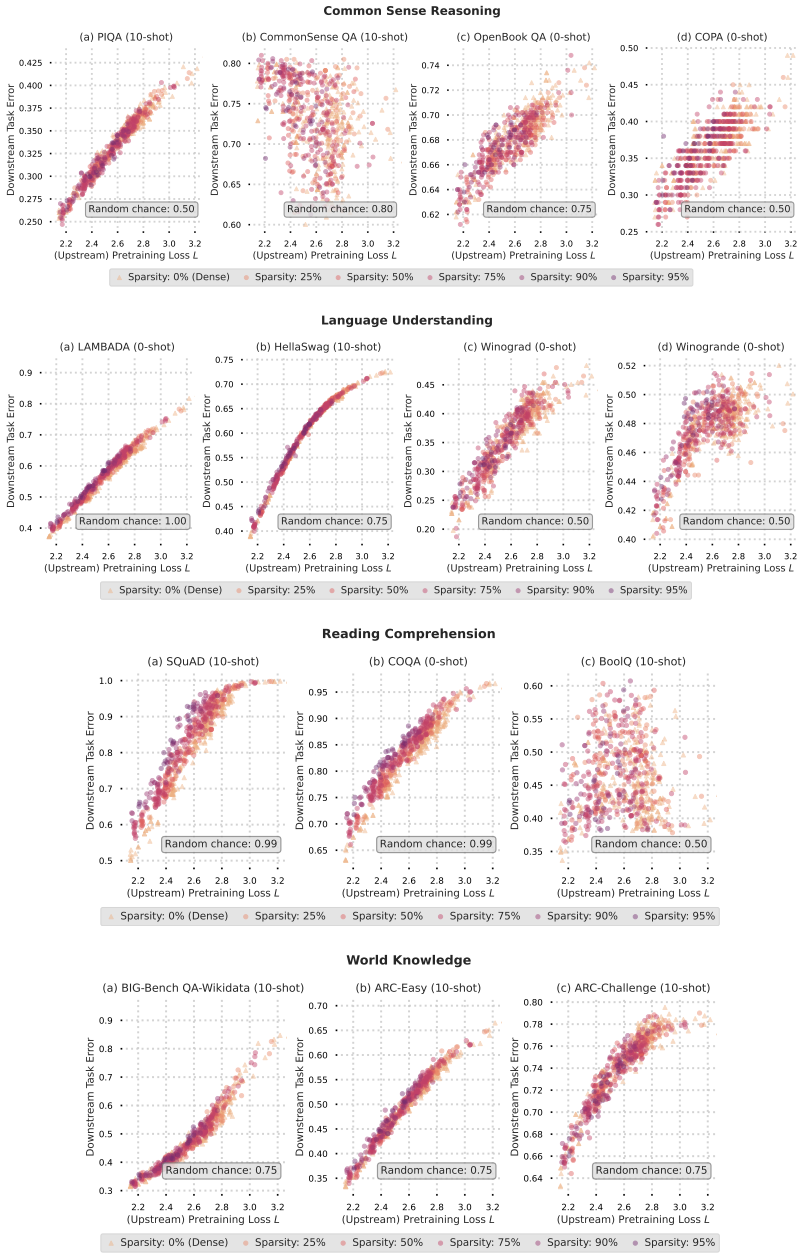

Figure 9: **Downstream task performance vs. upstream pre-training loss.** Each subplot shows the relationship between upstream pre-training loss (x-axis) and downstream task performance (y-axis) for a specific task. Similar to our results in Section 4, we find that the MoE sparsity level does not change the relationship between upstream pre-training loss and downstream task performance.

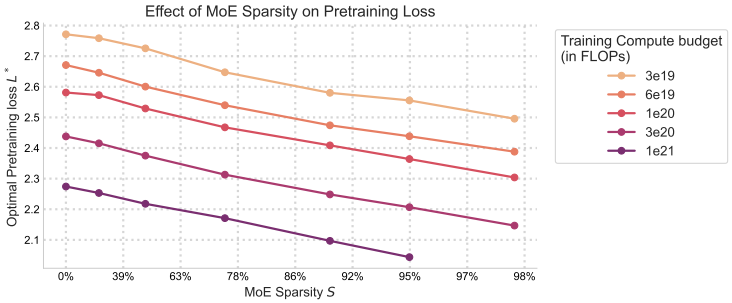

Figure 10: **Effect of MoE sparsity on pretraining loss across different training compute budgets**. As sparsity increases, the validation loss decreases for all compute budgets, with larger budgets (darker lines) achieving lower losses at each sparsity level. This trend is consistent with the findings from Section 3, demonstrating that increasing sparsity reduces the optimal pretraining loss across all compute budgets.

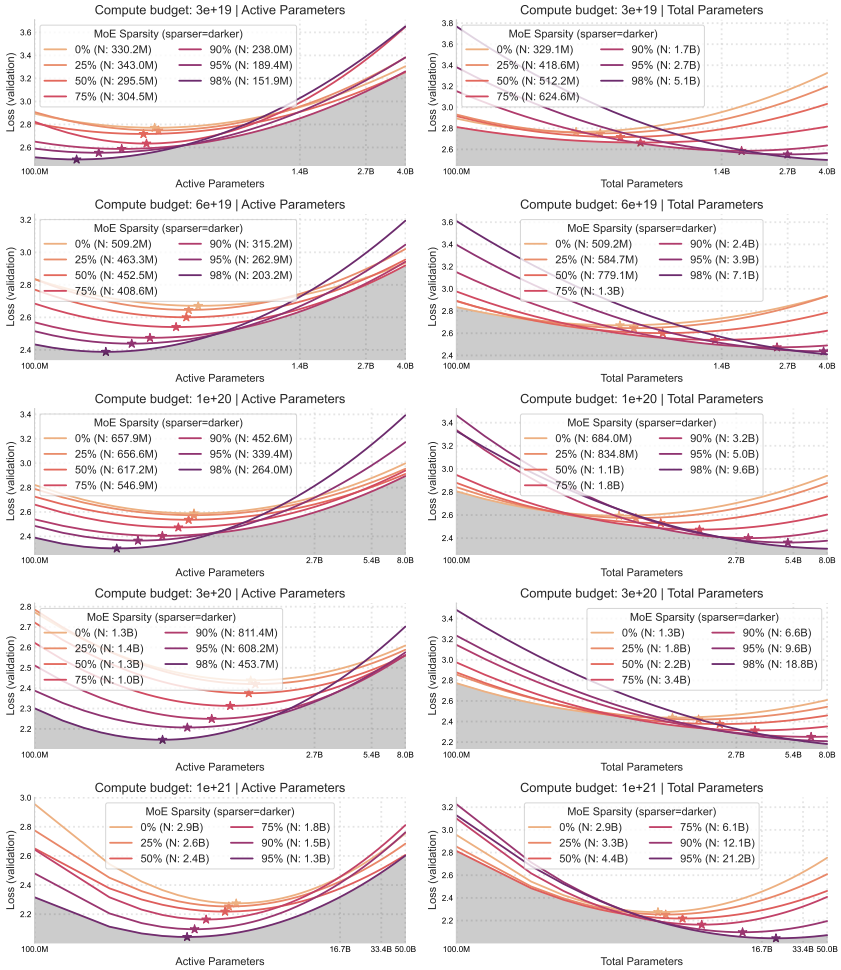

Figure 11: **Effect of MoE sparsity on optimal total and active parameters across different training compute budgets.** Each row shows the change in total and active parameters as a function of sparsity level for fixed training budgets. Increasing sparsity leads to an increase in the optimal total parameters while reducing the optimal active parameters, consistent with our findings in Section 2 (Figure 5). Larger training compute budgets result in higher optimal (total and active) parameters across all sparsity levels.

G Incorporating Sparsity into Scaling Laws

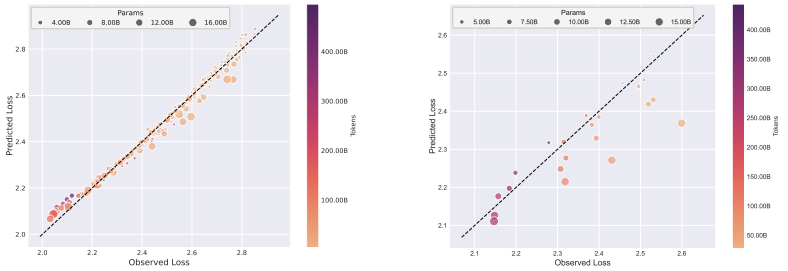

(a) Fit on data used to estimate coefficients.

(b) Validating scaling law on held-out dataset.

Figure 12: Scaling law fit on data obtained from training compute-optimal models. Figure (a) shows fit on data used to estimate coefficients for Equation 2 while (b) validates the estimated coefficients on a held-out dataset. All $S = 0.98$ data points were excluded from the fitting process to provide an out-of-sample validation. The dashed lines represent equal loss values.

G.1 Scaling Law for Dense Models

The scaling laws proposed by Kaplan et al. (2020) provide a framework for predicting loss in dense models by establishing a power-law relationship between loss L, number of parameters N and dataset size D, where N and D interact linearly. Formally, the relationship is given by:

$$L(N, D) = \frac{a}{N^{\alpha}} + \frac{b}{D^{\beta}} + e \tag{8}$$

Here, the term N^{α} captures the inverse relationship between model size and loss, where an increase in model size N leads to a reduction in loss. The exponent α quantifies the rate of this decrease; a larger α suggests a steeper reduction in loss with increasing model size. Similarly, the term D^{β} indicates the impact of dataset size D on loss, with larger datasets contributing to lower loss values. The exponent β measures this relationship, where a larger β implies a greater benefit from increased data. The constant e represents an asymptotic minimum for the loss, as both model size and dataset size approach infinity.

G.2 Fitting Coefficients to Scaling Laws for Sparsity

By incorporating sparsity into the scaling law equation, we can eliminate the need for parameters specific to MoEs, such as the total and active number of experts. Indeed, as Frantar et al. (2024) demonstrates, this same equation, Equation 2, continues to hold under a different mechanism for introducing sparsity—weight sparsity—where individual neural network connections are pruned.

We use the recipe described by Hoffmann et al. (2022) and use the L-BFGS algorithm to fit the coefficients in Equation 2 using a Huber loss with $\delta = 10^{-3}$. The optimal coefficient values are found via a grid search with values described in Table 2. The results of data fitting and validation are shown in Figure 12. The estimated values are shown in Table 3 in Appendix G.

G.3 Hyperparameters and Estimated Coefficients

Table 2 shows the parameters used to initialize L-BFGS used to fit the proposed parametric scaling law given in Equation 2. Table 3 shows the estimated parameters for the parameteric model. We use a held out dataset that consists of data points for models with sparsity value $S = 0.98$ to validate the performance of the estimated model coefficients. The mean squared error and the Huber loss error on the dataset used to fit the model is 0.00056 and 0.0036 respectively and 0.0058 and 0.0011 respectively on the out-of-sample validation set.

Table 2: Initial values used to estimate coefficients in Equation 2.

coefficients	initial values
$\log(a)$, $\log(b)$, $\log(c)$, $\log(d)$	$[0, 10, 20]$
α, β, γ	$[0, 0.25, 0.5, 0.75, 1, 1.25]$
λ, δ	$[-1, -0.5, 0, 0.5, 1]$
$\log(e)$	1.5

Table 3: Estimated values for coefficients in Equation 2.

coefficient	estimate
α	0.5962
β	0.3954
λ	-0.1666
δ	0.1603
γ	0.1595
a	16612.50
b	5455.67
c	0.4598
d	17.26
e	0.94

H Discussion

Our findings amplify the findings of Ludziejewski et al. (2024) and further justify the effort to work toward MoEs with experts larger in number and smaller in size (He, 2024). For downstream tasks which their performance is predictable given the pretraining loss (i.e., perplexity), sparsity potentially provides efficiency gains both during pretraining and inference. Here is a summary of our observations as discussed in Sections 2 to 5 :

- **Larger, Sparser Models Perform Better under a Fixed Compute Budget:** When memory and communication overheads are disregarded, increasing sparsity while proportionally expanding the total number of parameters consistently leads to a lower pretraining loss, even when constrained by a fixed training compute budget (see § 2).
- **Optimal Sparsity for Fixed Model Size:** For any given number of parameters and under a fixed training compute budget, model performance as a function of sparsity exhibits a parabolic pattern, reaching its peak at an optimal sparsity level (see §F.2). Specifically, the optimal sparsity:
  - Increases with the total number of parameters approaching 1.0 for larger models. i.e., if a model is relatively small for a given training compute budget, sparsifying it more than a threshold will hurt its performance. On the other hand, if a model is relatively large for a given compute budget, further sparsifying it helps as it leads to increase in the number of tokens the model is trained on under the given training budget constraints (see §F.2).
  - Increases across all model sizes as the training compute budget increases (see §F.3 and §F.4).
- **Effect of Sparsity on Scaling Laws for Optimal Model Size:** For any specific sparsity level, performance of the models as a function of their size exhibits parabolic behavior under a fixed training compute budget. i.e., the model reaches its optimal performance at a vertex, that indicates optimal model size. Under these conditions:
  - The optimal active number of parameters decreases as the sparsity level increases, leading to smaller FLOPs per example and more efficient inference even though the total number of parameters increases (see §F.1).
  - While the trend of increasing active number of parameters is similar across all training compute budgets; the optimal active number of parameters decrease more rapidly with sparsity as the training compute budget increases (see §3).
- **Effect of Sparsity on Downstream Performance:** For most downstream tasks, models with similar pretraining perplexity have similar downstream task performance regardless of sparsity. For reading comprehension tasks (e.g., CoQA (Reddy et al., 2019), SQuAD (Rajpurkar et al., 2018)), denser models perform better, potentially due to their higher inference-time compute than a perplexity-matched sparse model. Strategies to increase inference time compute dynamically (Wei et al., 2022b; Goyal et al., 2024) may address this gap.
- **Parametric Scaling Law:** We propose a parametric form for scaling laws that accounts for sparsity. The model coefficients are estimated using the empirical data obtained by training compute-optimal models. An interesting observation from Appendix G is that the exponent for sparsity term λ is negative which is consistent with our intuition that sparser models lead to a lower perplexity.

I Conclusion

In this paper, we investigated the optimal trade-off between parameters and compute per example for maximizing model capacity. Our findings indicate that sparsity, as a knob that controls FLOPs per example in MoEs, is a powerful mechanism for optimizing model performance under constrained training compute budgets. By balancing the total number of parameters, compute, and sparsity, MoEs can be scaled more effectively. These insights provide valuable guidance for scaling language models, especially for MoEs, where the trade-offs between parameters and FLOPs must be carefully managed.

MoEs were originally introduced to allow increasing model capacity without a significant increase in inference cost. Our experiments show that under fixed total training compute budget increasing sparsity in MoEs leads to smaller FLOPs per example, higher number of parameters, and lower pretraining loss simultaneously. In other words, in the context of MoEs, if there are no constraints on the total number of parameters, increasing the capacity of the model through parameter count seem to be the optimal strategy if lower pretraining loss is the main goal. On the other hand, when comparing how well the pretraining performance transfers to various downstream tasks, denser models seem exhibit better transfer performance on certain types of task that potentially rely on deeper processing of the input vs the knowledge stored in the parameters of the model. This potentially signals the importance of the role of FLOPs per example in increasing the capacity of the model during inference. This observation reveals an interesting direction to improve the performance efficiency of MoEs at inference time.

Future work will focus on determining the optimal balance between FLOPs per example and parameter count, with an emphasis on conducting in-depth analyses of model performance across diverse downstream tasks. A key direction will involve exploring strategies to balance parameter allocation and computational demands to minimize inference costs. Developing scaling law studies to identify optimal approaches for achieving efficiency and performance during inference represents a critical area for further investigation.

Another important avenue will be to examine how the findings on the role of sparsity in MoEs generalize to architectures or approaches that employ different mechanisms for independently adjusting FLOPs per example and the number of trainable parameters. Additionally, an intriguing direction for future exploration is the study of scaling behaviors in models that enable negative sparsity values through parameter sharing.

J Limitations

In our analysis, similar to other scaling law studies (Kaplan et al., 2020; Hoffmann et al., 2022), we have measured the costs for both training and inference exclusively in terms of FLOPs. While there may be discrepancies between actual computational costs and theoretical FLOPs due to hardware specifications, infrastructure, and implementation details, it is reasonable to abstract away from these factors when comparing similar models under fixed conditions. However, an important aspect not accounted for in this study is the cost associated with memory usage and communication overhead, which could potentially increase as we raise the sparsity level. Incorporating these factors is challenging because they are highly dependent on the hardware used. To address this limitation to some extent, in Appendix F.2 we investigate the optimal sparsity level under the setting where total number of parameters is fixed.

Despite the limitation with using an approximate method to quantify FLOPs, our findings highlight the importance of investing in methods to enhance the efficiency of sparse Mixture-of-Experts models. By increasing model capacity through additional parameters while minimizing per-unit computation costs, these models have the potential to improve both efficiency and performance. The availability of GPUs with larger memory, for e.g., the recently introduced H200 GPU chip with 141 GB of memory as well as improving the efficiency of training and deployment pipelines (NeMo Authors, 2025) suggest that there is significant interest in developing efficient implementations for MoEs.